



CM-P00071916

ISR PERFORMANCE REPORTRun 539 - 21 October 1974Run 543 - 25 October 1974Rings 1 and 2 - 26 GeV/cFirst and second test of the steel low- β sectionGeneral conclusion

The section behaved as expected :

- Reduction of ≈ 2.3 in the beam height which was reflected in the luminosity figures obtained :

$$9.76 \mu\text{b}^{-1} \text{s}^{-1} \text{ with } 12.136^{\text{A}} \times 12.774^{\text{A}} \text{ and } h_{\text{eff}} = 1.58 \text{ mm}$$

$$\text{and } 10.2 \mu\text{b}^{-1} \text{s}^{-1} \text{ with } 12.133^{\text{A}} \times 14.046^{\text{A}} \text{ and } h_{\text{eff}} = 1.66 \text{ mm.}$$

- Outside the section the perturbation of the horizontal closed orbit is small; it is largest when $\Delta p/p$ and Q' are maximum but still less than 2 mm peak-to-peak. The dependence of the CO with $\Delta p/p$ is smaller than that which results from the use of large Q' (2.5). The effect on the available aperture can be eliminated by applying a common orbit correction at both ends of the aperture.
- The section gave an additional 4 mm peak-to-peak vertical orbit distortion in Ring 2, and probably less in Ring 1. There is no clear relation between these distortions and $\Delta p/p$, which will prevent applying any simple correction. A part of this effect could be due to a small misalignment of the Q3 quadrupole which has been detected and corrected in Ring 2. In any case, the overall 5.5 mm peak-to-peak distortion measured in Ring 1 is a quite good value.
- When stacking, we hit a brickwall limit as we had no feedback and a working line of large Q' but very close to the 9th integers. After having lost the beams in the region of 9 A, we stacked up to 14. A in the full aperture during Run 543 and even 15.1 A during Run 539.

These limitations agree with a scaling from the 8C working line and will be hopefully overcome by using the feedback system.

- The dI/dt of 3 to 4 ppm in Ring 2 and 10 to 15 ppm in Ring 1 with currents of 12 to 14 A are quite normal because of the presence of 7th order resonances in the stack. The difference between the two rings which reflects in the transverse Schottky scans is unexplained.

History of Run 539

- B pulse increased by 6 % in order to inject at $\bar{x} \approx -30$ mm
- Set-up of the working line LB1 (see Figures 1 and 2) with small Q' ($Q'_h = Q'_v = 1.2$) - this to avoid the problematic CO instability which is encountered by the AGS program for $Q' > 1.6$.
- Injection with the low- β quadrupoles off - No problems - CO measured at 3 radial positions.
- Verification of the sign of the gradients in the quadrupoles by the effect on the Q values of a 5 % excitation of each of them - No problems.
- Setting-up of the calculated currents : injection went immediately well without retouching the previous optimization - CO and Q measurements.
- Increase of the Q's to the nominal values of $Q'_h = Q'_v = 2.48$. No problems for injection, acceleration, etc. (the instability when using AGS is due to the program and not to the machine). Slight reoptimization of injection.
- Vertical profile measurements by K. Potter with the I5 and I7 scrapers with single PS pulses at CO and + 40 mm in Ring 1.
- Tests of stacking with a theoretical density of 400 mA/mm (the actual density was probably less as we had a large unscraped spill out).
- First test of the I7 monitor at an intermediate stage with 13.4 A (Ring 1) and 8.04 (Ring 2).

History of Run 543

- B pulse increased by $\approx 1\%$ to inject at $\bar{x} = -39$ mm.
- Set-up of the nominal Q' working line LB2 (see Figures 1 and 2).
CO measurements with the quadrupoles off in Ring 2.
- Nominal currents - as for Run 539 - in the quadrupoles. Injection optimization. CO measurements.
- Calibration of the new I7 vertical bumps by K. Potter with the I7 scraper in both rings at CO and $\bar{x} = 40$ mm.
- Calibration of the I7 monitor using unshaved 4A stacks on CO (K. Potter)
- Tests of stacking with a density of 240 A/mm. Luminosity and dI/dt measurements. Schottky scans.

Working lines measurements

Figures 1 and 2 give the final Q-values for the normal working line (LB2) and for the reduced Q' working line (LB1). The nominal currents are in the file LB2 (Figure 3). For the effect of the low- β section on the Q-values, the relevant figures are (Run 539) :

	Lenses off	Lenses on
Inj. - 28.2	$Q_h = 8.875$ $Q_v = 8.641$	$Q_h = 8.863$ $Q_v = ?$
+ 3.9 mm	$Q_h = 8.894$ $Q_v = 8.664$	$Q_h = 8.880$ $Q_v = 8.856$
+ 39.8 mm	$Q_h = 8.919$ $Q_v = 8.693$	$Q_h = 8.901$ $Q_v = 8.883$

The Q-shifts on CL are $\Delta Q_h = -0.014$ and $\Delta Q_v = +0.192$ to be compared to the theoretical values of -0.0147 and $+0.1945$, respectively.

CO measurements

a) Working line with reduced $Q'_{h,v}$ - LB1 - Ring 2 - Run 539

The main results are given in Table 1 for the lenses "on" (normal figures) and off (values in brackets).

Values in mm	at $\bar{x} \approx -29$ mm	at $\bar{x} \approx 0$	at $\bar{x} \approx 39$ mm
\bar{x}	-29.0 (-29.2)	- 1.1 (3.2)	39.3 (39.2)
Δx_{RMS}	1.3 (1.2)	1.5 (1.3)	2.0 (2.1)
$\Delta x_{\text{peak-to-peak}}$	5.0 (5.1)	7.1 (6.2)	8.1 (8.7)
\bar{y}	- 0.1 (-0.1)	-0.1 (-0.1)	-0.2 (-0.2)
Δy_{RMS}	0.9 (0.8)	0.9 (0.9)	1.7 (1.0)
$\Delta y_{\text{peak-to-peak}}$	4.6 (3.6)	4.8 (4.2)	7.3 (4.7)

Table 1

b) Working line with nominal $Q'_{h,v}$ - LB2 - Rings 1 and 2 - Run 543

The following main results were obtained :

Values in mm	at $\bar{x} \approx -40$ mm	at $\bar{x} \approx 0$	at $\bar{x} \approx 39$ mm
\bar{x}	-39.8 (-39.9)	- 5.9 (-0.3)	40.4 (38.8)
Δx_{RMS}	2.1 (1.4)	1.4 (1.3)	3.1 (2.7)
$\Delta x_{\text{peak-to-peak}}$	8.4 (6.3)	6.2 (6.3)	11.9 (10.6)
\bar{y}	0.0 (0.0)	0.0 (-0.1)	-0.1 (-0.1)
Δy_{RMS}	1.5 (0.8)	1.2 (0.9)	1.6 (1.0)
$\Delta y_{\text{peak-to-peak}}$	7.3 (3.3)	5.9 (3.6)	7.0 (4.5)

Table 2 : Ring 2

Values in mm	at $\bar{x} \approx -40$ mm	at $\bar{x} = 0$	at $\bar{x} \approx 39$ mm
\bar{x}	-39.8	-1.2	39.3
Δx_{RMS}	2.9	1.4	3.8
$\Delta x_{\text{peak-to-peak}}$	12.0	5.4	13.0
\bar{y}	0.3	0.2	0.1
Δy_{RMS}	1.2	1.1	1.3
$\Delta y_{\text{peak-to-peak}}$	5.2	4.7	5.5

Table 3 : Ring 1

Figure 4 shows the horizontal CO distortions around the rings with the lenses "on".

c) Discussion

The discrepancy between the normal values and those in brackets gives a measure of the quality of the matching of the section to the rest of the machine.

- In the horizontal plane the matching is very good for the small Q' working line ($\Delta x_{\text{RMS}} < 0.2$ mm) and slightly worse for $Q'_{h,v} = 2.48$ ($\Delta x_{\text{RMS}} < 0.7$ mm for extreme $\Delta p/p$). This fact is due to the absence of a sextupolar component in the low- β quadrupoles - the matching being done for the Q_h, Q_v of CL.
- When the lenses are "on", the horizontal closed orbit distortions vary with $\Delta p/p$ and are maximum for extreme $|\Delta p/p|$, as can be clearly seen in Figure 4. In addition to the mismatching, this effect includes the variation of the distortions with $\Delta p/p$, which is known to be present even in a perfectly periodic machine when large Q 's are used. In any case, the phase and the amplitude of the main harmonic of the distortion is roughly the same for opposite $\Delta p/p$, which means that a common correction can be applied at the two ends of the aperture. The distortion on the CL will be increased but this is of little consequence.
- In Ring 2, the comparison of the y normal or in brackets shows that the section introduces a certain vertical orbit distortion ($\Delta y_{\text{RMS}} < 0.7$ mm). The distortion is maximum for extreme $\Delta p/p$ but the dependence with Q' is not clear. A small vertical misalignment (2/10 mm) of the Q3 quadrupole has been found in Ring 2, which could explain a part of this effect and the fact that the distortions are larger in Ring 2 than in the other Ring. There is no evident correlation between the distortions at the sides of the aperture (Figure 5), which means that a classical correction with the H-magnets cannot be used. These distortions are small enough to be disregarded for the time being but we intend to analyse them in order to find what type of quadrupole misalignment (tilt and displacement) could explain them.

Vertical profiles of single PS pulses in I7 and I5 - Ring 1 - K. Potter

Figures 6 and 7 give the profiles for pulses deposited at CL and at $\bar{x} = 39$ mm in Ring 1, as measured with the I5 and I7 scrapers. Beam height ratios rather independent of \bar{x} were measured :

At CL : 2.37 ± 0.1 to be compared to $\sqrt{\frac{\beta_V^{I5}}{\beta_V^{I7}}} = \sqrt{\frac{15.7}{2.8}} = 2.368$

In the same experiment, the vertical position of the beam centers was found as follows :

	I5	I7
Central orbit	- 0.292 mm	0.245 to 0.251 mm
$\bar{x} = + 39$ mm	- 0.861 mm	0.146 mm

The corresponding tilts of the median plane are :

At I5 : $\frac{0.861 - 0.292}{39} \times \frac{\bar{\alpha}_p}{\alpha_{pinI5}} = 13$ mrad

At I7 : $\frac{0.248 - 0.146}{39} \times \frac{\bar{\alpha}_p}{\alpha_{pinI7}} = 1.64$ mrad.

The value of 13 mrad is about twice that which is usually measured with a periodical machine.

Calibration of vertical bumps in I7 - Run 543 - K. Potter

As the vertical phase advance in I7 is radically modified by the low- β section, special 4-magnet bumps have been calculated by A. Verdier and myself using 2 new special H magnets installed in the intersection I7 itself.

- For Ring 1 : 1H 717 1H 701 1H 653 1H 617
- For Ring 2 : 2H 648 2H 664 2H 716 2H 752

The calibration made by K. Potter using the I7 scraper to kill single PS pulses on CL or at $\bar{x} = + 40$ mm gave the following results :

./...

Radial position	Vertical bump/mm	Scraper results	
0	- 1	- 1.247	1.022 mm/applied mm
	+ 1	0.797	
+ 40	- 1	- 1.250	0.927 mm/applied mm
	+ 1	0.604	

The radial dependence of bump height - 9 % for $\bar{x} = + 40$ mm is about twice as large as that usually measured with the FP or 5C line with a periodic machine. Is it an effect of the ELSA working line ?

In Ring 2, the calibration gave obviously wrong results (1.19 mm/applied mm on CL and 1.36 mm/applied mm at $x = + 40$ mm) due to a mistake in the bumps coefficients.

Calibration of the I7 monitor constant - Run 543 - K. Potter

Two stacks on CL of 4.57 A (Ring 1) and 4.65 A (Ring 2) were made and steered vertically in I7 to draw a luminosity curve and derive the monitor constant. Only Ring 1 - with the correct bumps - was moved (see Figure 8).

Stacking - Luminosity figures - Decay rates

- Run 539

With the following conditions : $\Gamma = 0.5$, $\Delta f = 7$ Hz, top at + 40 mm : Corrections of the average incoherent Q-shift every 6 A as for the 5V26 working line. No shaving but only 50 mA left in the final bucket. No periodic removal of the spill out as for the next run. Density : 400 mA/mm of aperture : we lost beam 2 during alternate stacking at 8.85 A (8.92 A in Ring 1) after having applied successfully the first Q-correction in both beams at ≈ 6 A. Stacking in Ring 1 was continued to 13.4 A and was stopped without applying the second correction. Ring 2 stacking was re-started and stopped at 8.04 A to allow the first preliminary luminosity measurements in I7 (K. Potter). Stacking was then continued in Ring 2 without applying any Q-correction up to 15.1 A intensity at which we lost the beam - probably because of the vertical brickwall type instabilities which were clearly seen on the scope.

- Run 543

With the following conditions : $\Gamma = 0.5$, $\Delta f = 7$ Hz, top at + 40 mm :
 Corrections of the complete incoherent Q-shift every 4 A as for the 8C26 working line. Shaving to ≈ 45 mA in order to have ≈ 30 mA in the final bucket. Removal of the spill out prior to each Q-correction.
 Density : 240 mA/mm of aperture. Alternate stacking went well up to 10.4 A in Ring 2 (10.7 A in Ring 1) where we lost beam 2 after a period of vertical instabilities on the scope. The two first Q-corrections had been applied without loss at 4 and 8 A. Then stacking was continued in Ring 1 up to saturation - against the shaver - with a final intensity of 11.7 A. Ring 2 was restacked in the same conditions up to 10.15 A.
 Luminosity and decay rates were measured :

$$\begin{aligned} (1) \quad & 9.182^{\text{A}} \text{ (R1)} \times 10.183^{\text{A}} \text{ (R2)} \quad 6.09 \mu\text{b}^{-1} \text{ s}^{-1} \quad h_{\text{eff}} = 1.53 \text{ mm} \\ (2) \quad & 11.606^{\text{A}} \text{ (R1)} \times 10.151^{\text{A}} \text{ (R2)} \quad 7.63 \mu\text{b}^{-1} \text{ s}^{-1} \quad h_{\text{eff}} = 1.54 \text{ mm} \end{aligned}$$

With these latter conditions, the dump block centered and the injector withdrawn, the decay rate over 10 minutes were about :

$$14 \text{ ppm mm}^{-1} \text{ in Ring 1 and } 3 \text{ ppm mm}^{-1} \text{ in Ring 2.}$$

Then we continued to stack to the maximum in both rings. The 3rd Q-correction was applied successfully at 12. A; we reached saturation at 12.134 A in Ring 1 after withdrawing the shaver and we stopped at 14.046 A in Ring 2 without saturation. The following luminosities have been measured :

$$\begin{aligned} (3) \quad & 11.602^{\text{A}} \text{ (R1)} \times 12.047^{\text{A}} \text{ (R2)} \quad 9.03 \mu\text{b}^{-1} \text{ s}^{-1} \quad h_{\text{eff}} = 1.55 \text{ mm} \\ (4) \quad & 11.602^{\text{A}} \quad \times \quad 12.216^{\text{A}} \quad \quad \quad 8.94 \quad \quad \quad 1.58 \\ (5) \quad & 12.136^{\text{A}} \quad \times \quad 12.774^{\text{A}} \quad \quad \quad 9.76 \quad \quad \quad 1.58 \\ (6) \quad & 12.133^{\text{A}} \quad \times \quad 14.046^{\text{A}} \quad \quad \quad 10.2 \quad \quad \quad 1.66 \end{aligned}$$

The decay rates measured with conditions (4) and with the inflector out and the dump block centered were :

$$14 \text{ ppm mm}^{-1} \text{ in Ring 1 and } 4 \text{ to } 5 \text{ ppm mm}^{-1} \text{ in Ring 2.}$$

Discussion

In Run 543 with a density of 240 mA/mm, after having lost once a beam at 10.4 A, we stacked 14 A in the same ring, filling the whole aperture. This figure agrees with that which can be scaled from the 15 A which can be stacked without feedback on 8C26 working lines :

$$\text{Gain due to the } Q' \text{ ratio : } \frac{Q'_v \text{ELSA}}{Q'_v \text{8C}} = 1.55$$

Loss due to the proximity of $Q = 9$:

$$\sqrt{\frac{(9 - Q_v) \text{ELSA}}{(9 - Q_v) \text{8C}}} = 0.52 \text{ (at the stack top + 40 mm)}$$
$$= 0.68 \text{ (at the stack bottom - 13 mm)}$$

The intensity limit for the ELSA line will become 12 A or 15.8 A, whether it is calculated at the top of the stack (close to $Q_v = 9$ but where the Q'_v is increased by the incoherent Q -shift) or at the bottom (with opposite conditions).

The conditions of Run 539 were not clean enough to draw any conclusion as a large spill out remained in the aperture reducing the beam-density. However, the 15.1 A which have been stacked did not occupy the full aperture which tends to indicate that one can probably stack more intensity than that given by the previous scaling.

The dI/dt 's were quite good in Ring 2 (4 ppm mm^{-1}) and normal in Ring 1 (14 ppm mm^{-1}) as the stack was placed on the 7th order resonances which are known to give dI/dt 's of the order of 10 ppm min^{-1} with a normal machine (at least the resonances $n_1 Q_h + (7 - n_1) Q_v = 61$).

The discrepancy between the dI/dt 's of the two rings is not explained.

./...

Schottky Scans - Run 543 (Figure 9)

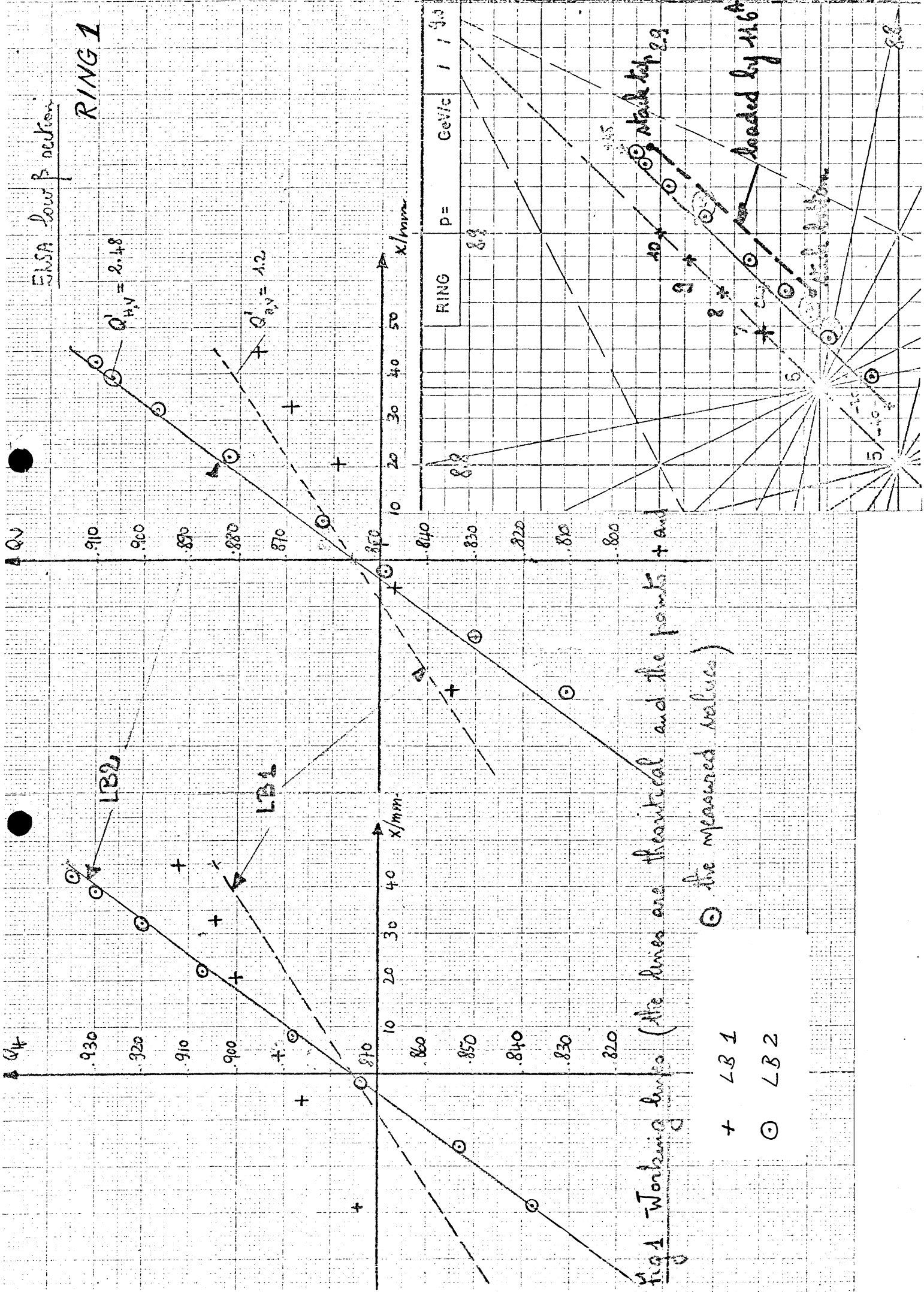
The longitudinal scans are flat and quite usual. The dip for Ring 1 at 11.6 A is probably due to an overscraping of the spill out at 8 A.

The transverse scans of Ring 2 are very smooth. On contrary peaks which could be identified with 6, 9 or 10th order resonances appear on the transverse scans of Ring 1. The loaded working lines are the same for the two rings (Figures 1 and 2). Why such a difference in the scan and the dI/dt 's ???

K. Brand

J.P. Gourber

S. Pichler



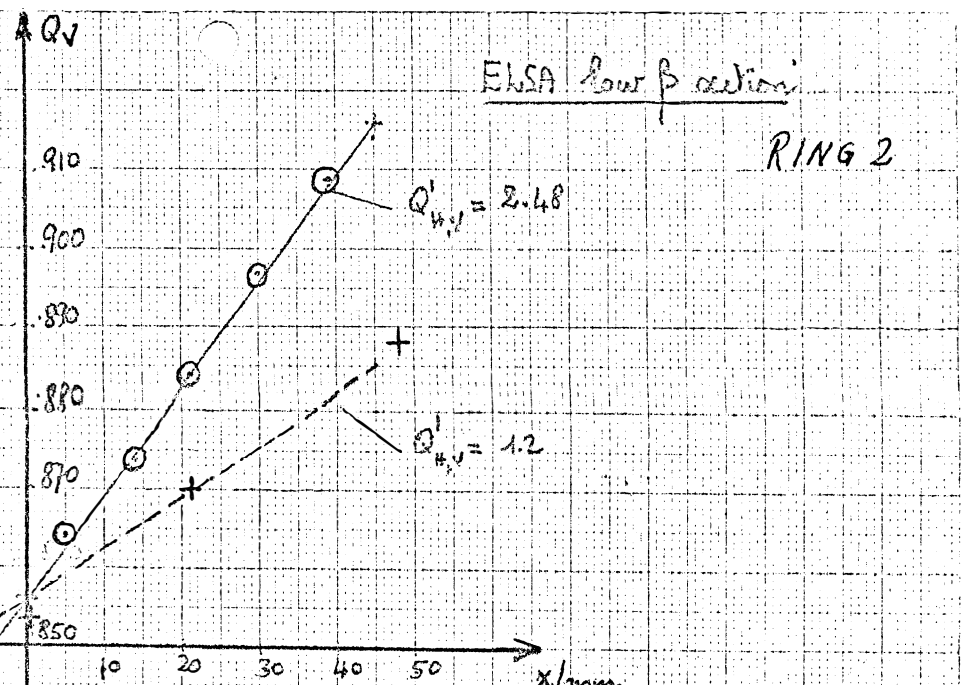
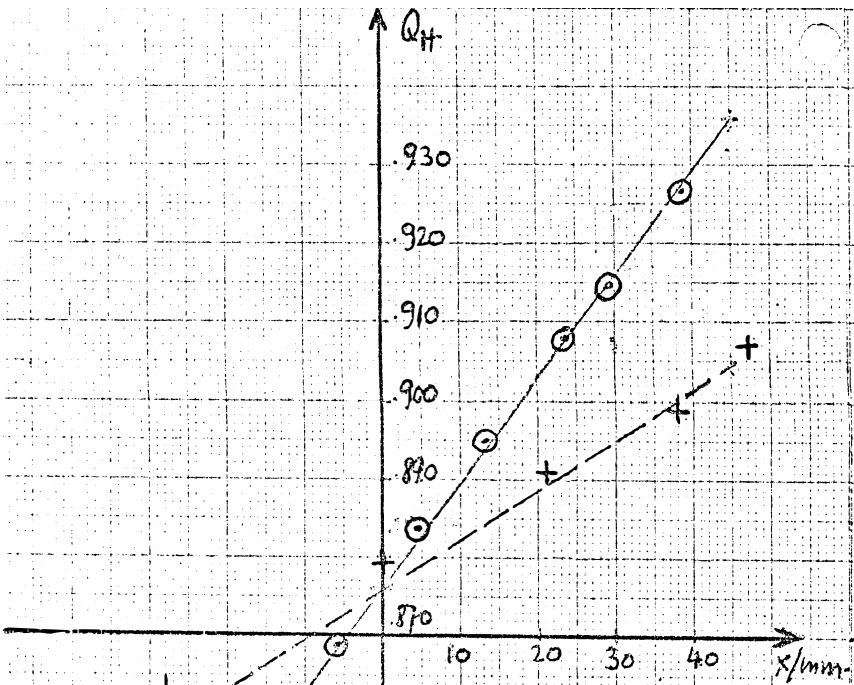


Fig 2 Working lines

- + LB 1
- ⊙ LB 2

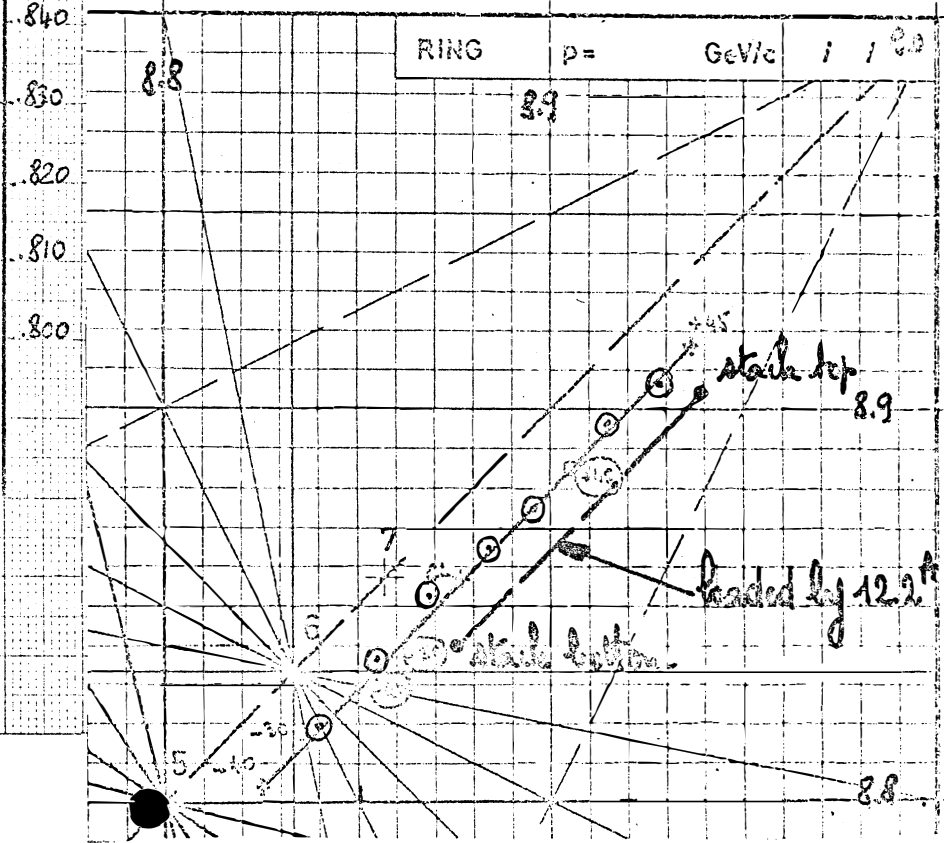


Fig 3 - Currents files

R1

```

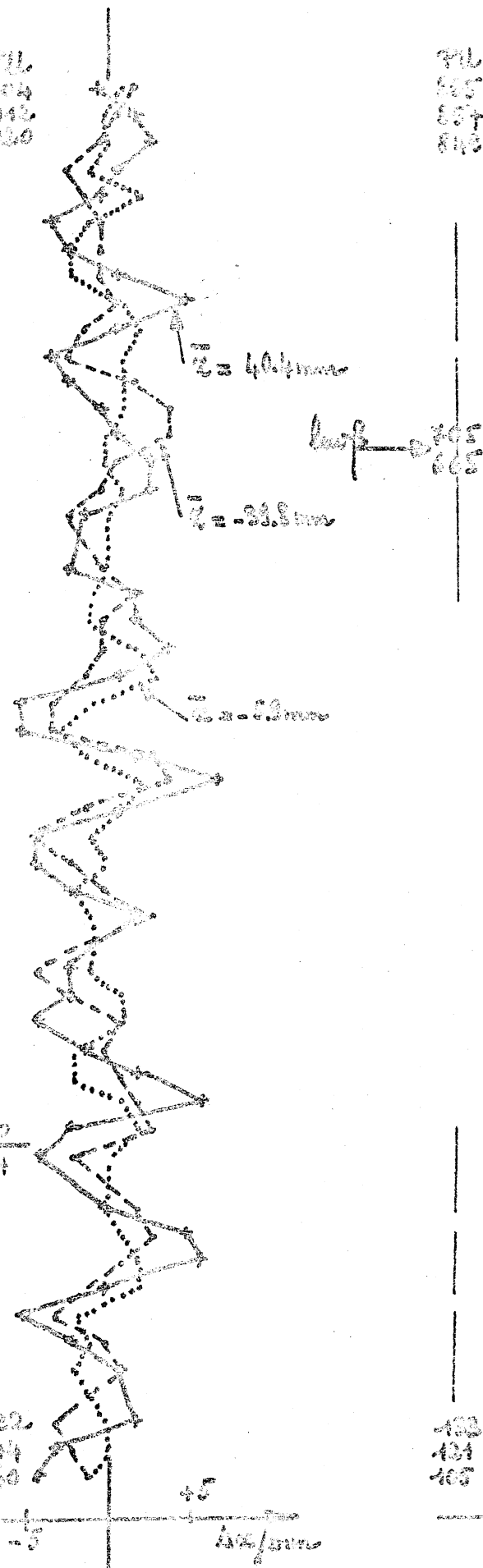
/XOUT (LB2,R1)      TIME:19H35M54S      DATE:74-10-21
/XKREE-RUN:539     XINP/XKREE-TIME:19H29M08S    DATE:74-10-21
/MAIN
/OT
 1CP      +47.29      1SF      +35.40      1SD      +34.52
/FF
 1PFF1    +45.24      1PFF2    +13.57      1PFF3     +4.54
 1PFF4    +15.75      1PFF5    +17.14      1PFF6    +17.07
 1PFF7    +18.51      1PFF8    +21.44      1PFF9    +24.73
 1PFF10   +23.85      1PFF11   +43.97      1PFF12   +38.53
 1PFD1    -31.03      1PFD2     -8.03      1PFD3     +3.32
 1PFD4     +7.06      1PFD5     +7.03      1PFD6     +6.96
 1PFD7     +8.91      1PFD8    +12.84      1PFD9    +16.21
 1PFD10   +11.13      1PFD11   +30.10      1PFD12   +27.71
/H
 1H717    -3.66      1H749A    +2.05      1H749B    +0.78
 1H817    -7.93      1H853     -2.93      1H117     -2.49
 1H149    -0.54      1H217     +0.51      1H253     -4.47
 1H317    -4.83      1H333    +10.28      1H349     +0.49
 1H417    -1.05      1H453     +3.05      1H517    +11.74
 1H549    -2.66      1H617     -1.37      1H653     -3.00
/CR
 1CR737   -5.30      1CR837   -5.20      1CR161    +7.93
 1CR529   -6.30
/ END OF DATA
    
```

R2

```

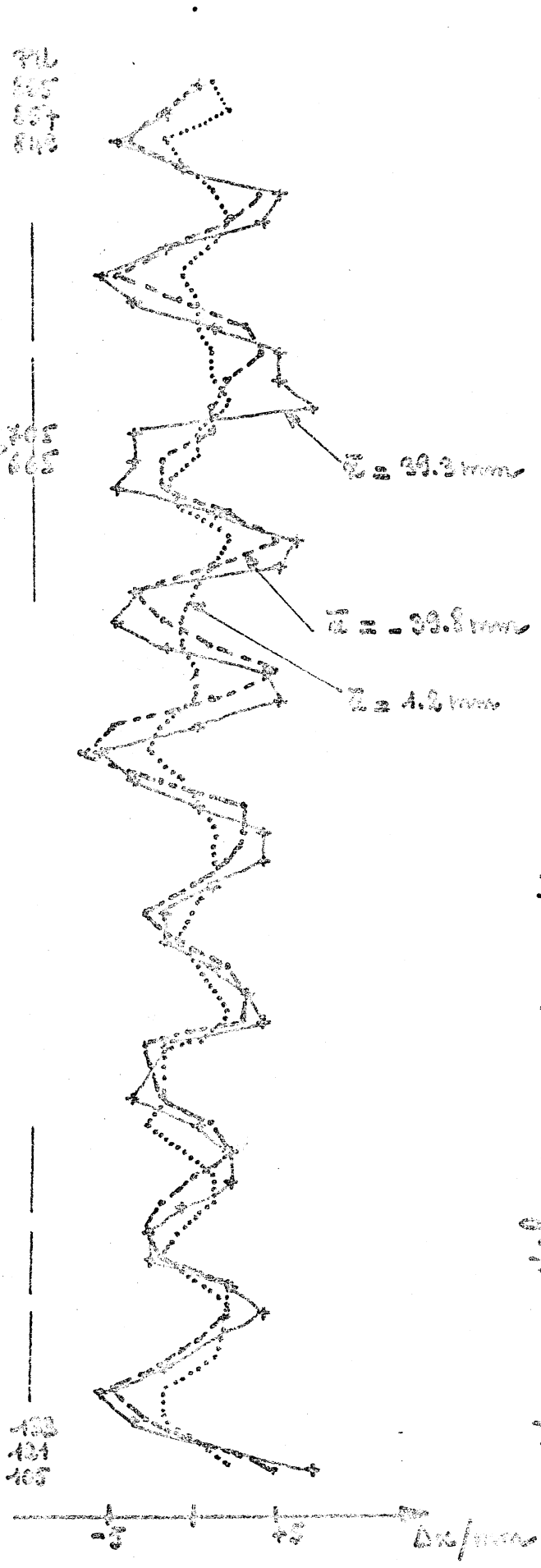
/XOUT (LB2,R2)      TIME:19H32M36S      DATE:74-10-21
/XKREE-RUN:539     XINP/XKREE-TIME:19H29M08S    DATE:74-10-21
/MAIN
/OT
 2CP      +42.65      2SF      +33.20      2SD      +32.45
 2Q1      -1.22
/FF
 2PFF1    +47.83      2PFF2    +14.79      2PFF3     +5.25
 2PFF4    +16.65      2PFF5    +18.04      2PFF6    +17.80
 2PFF7    +19.21      2PFF8    +22.02      2PFF9    +25.27
 2PFF10   +24.19      2PFF11   +44.29      2PFF12   +38.70
 2PFD1    -31.08      2PFD2     -8.06      2PFD3     +3.22
 2PFD4     +6.98      2PFD5     +6.98      2PFD6     +6.93
 2PFD7     +8.91      2PFD8    +12.79      2PFD9    +16.16
 2PFD10   +11.11      2PFD11   +30.08      2PFD12   +27.69
/H
 2H216A   +0.51      2H216B    +0.46      2H248     +0.81
 2H352    +3.27      2H316     -9.86      2H448     +3.27
 2H416    +2.69      2H552     +2.15      2H516     +1.12
 2H616    +9.91      2H632     +8.20      2H648     -1.61
 2H752    +2.91      2H716     -0.88      2H848     +4.86
 2H816    +1.90      2H152     -7.64      2H116     -4.13
/CR
 2CR236   -2.08      2CR260    +5.98      2CR308    -1.15
 2CR320    +2.69      2CR332    +3.34      2CR344    -4.81
 2CR356    +0.22      2CR404    +13.28     2CR420    -6.69
 2CR436    +4.32      2CR460    +2.54      2CR508    -5.25
 2CR520    +0.34      2CR532    +3.15      2CR556    -6.96
 2CR6
    
```

711
713
715
717



Run 92 with the leaf position
Working line with nominal Q_1^1
($Q_1^1 = Q_2^1 = 2.5$)

711
713
715
717



Run 91 with the leaf position
Working line with nominal Q_1^1
($Q_1^1 = Q_2^1 = 2.5$)

Fig 4 1/2 Cloud edge distance

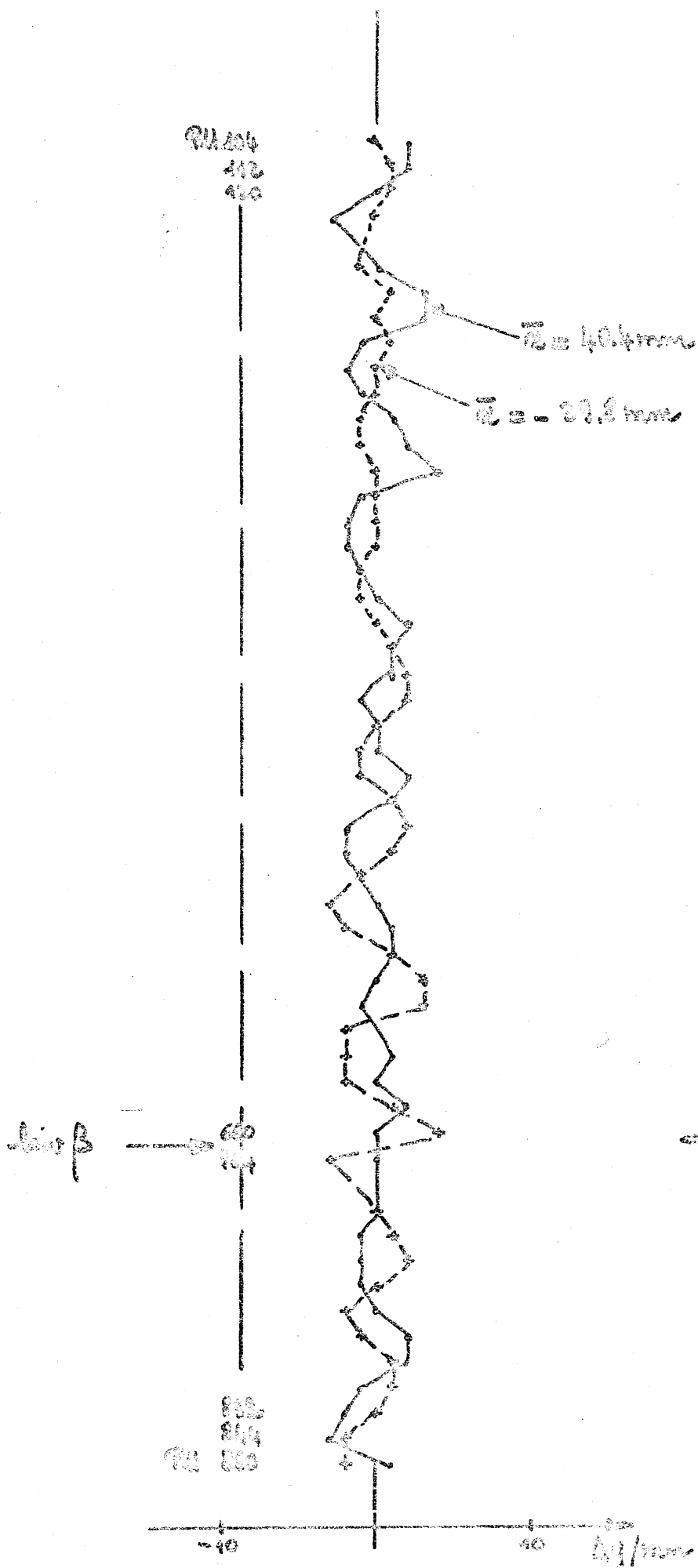


Fig. 7.1 cloud orbit distribution

Range with the loop orbit (vertical spread 0.4)

I_x

I_y

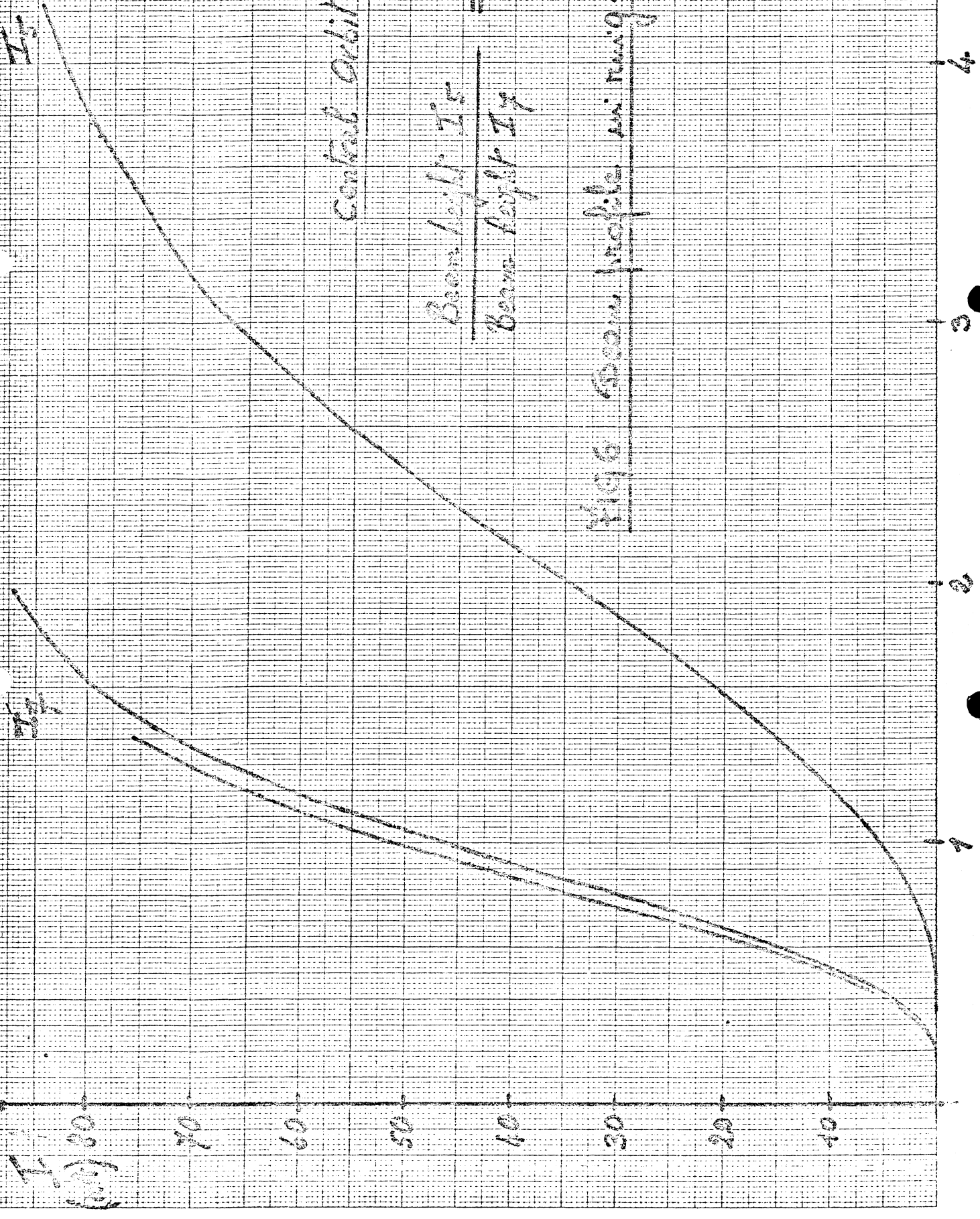
I_x (mm)

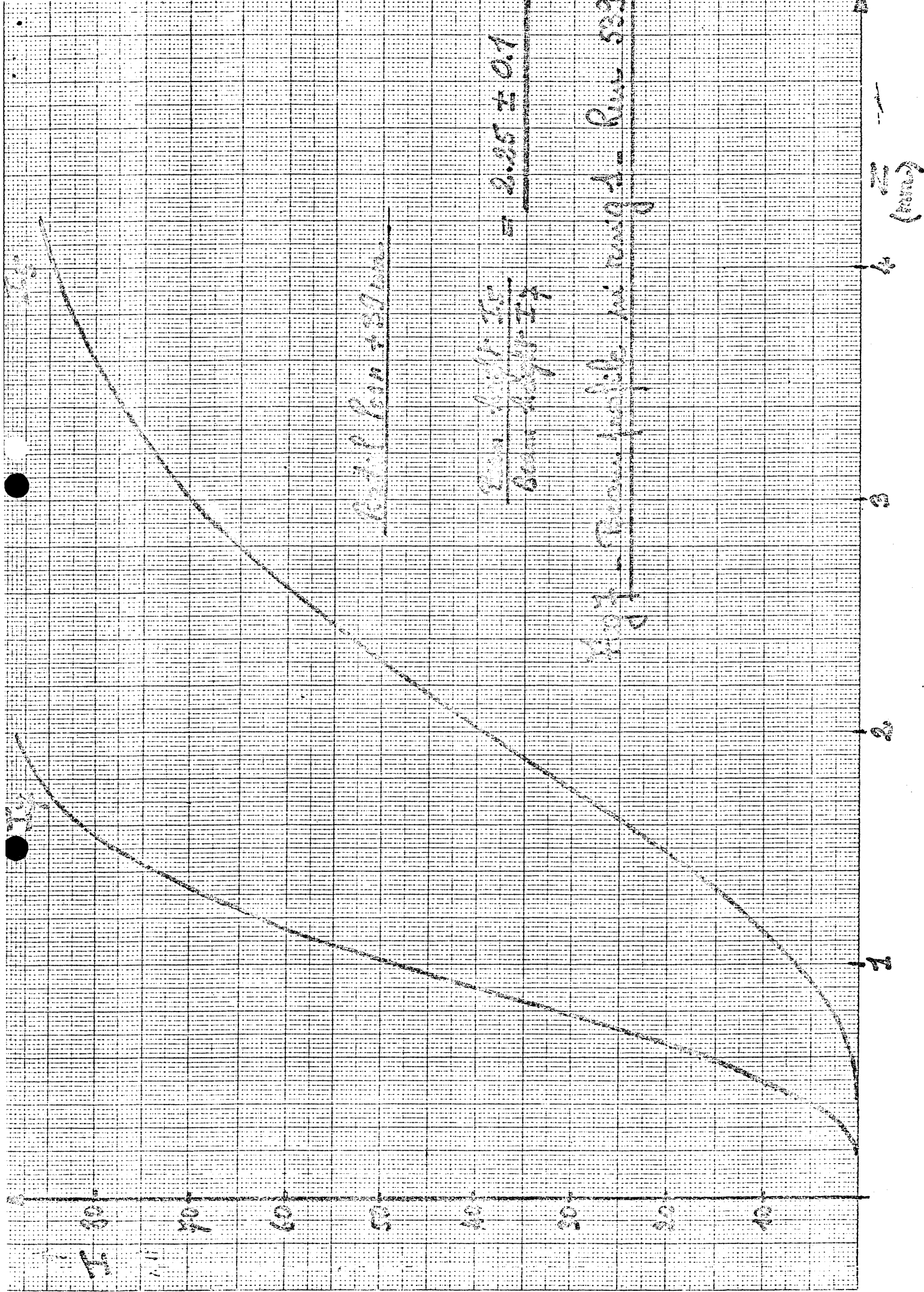
I_y (mm)

Control Orbit

$$\frac{\text{Beam height } I_x}{\text{beam height } I_y} = 2.37 \pm 0.1$$

Fig 6 Beam profile in mag 4 - Row 529





Handwritten notes at the top of the page, including a date "1/10/01" on the right.

Handwritten notes on the left side of the graph, including "1.00 / sec" and "1.00 / sec".

①

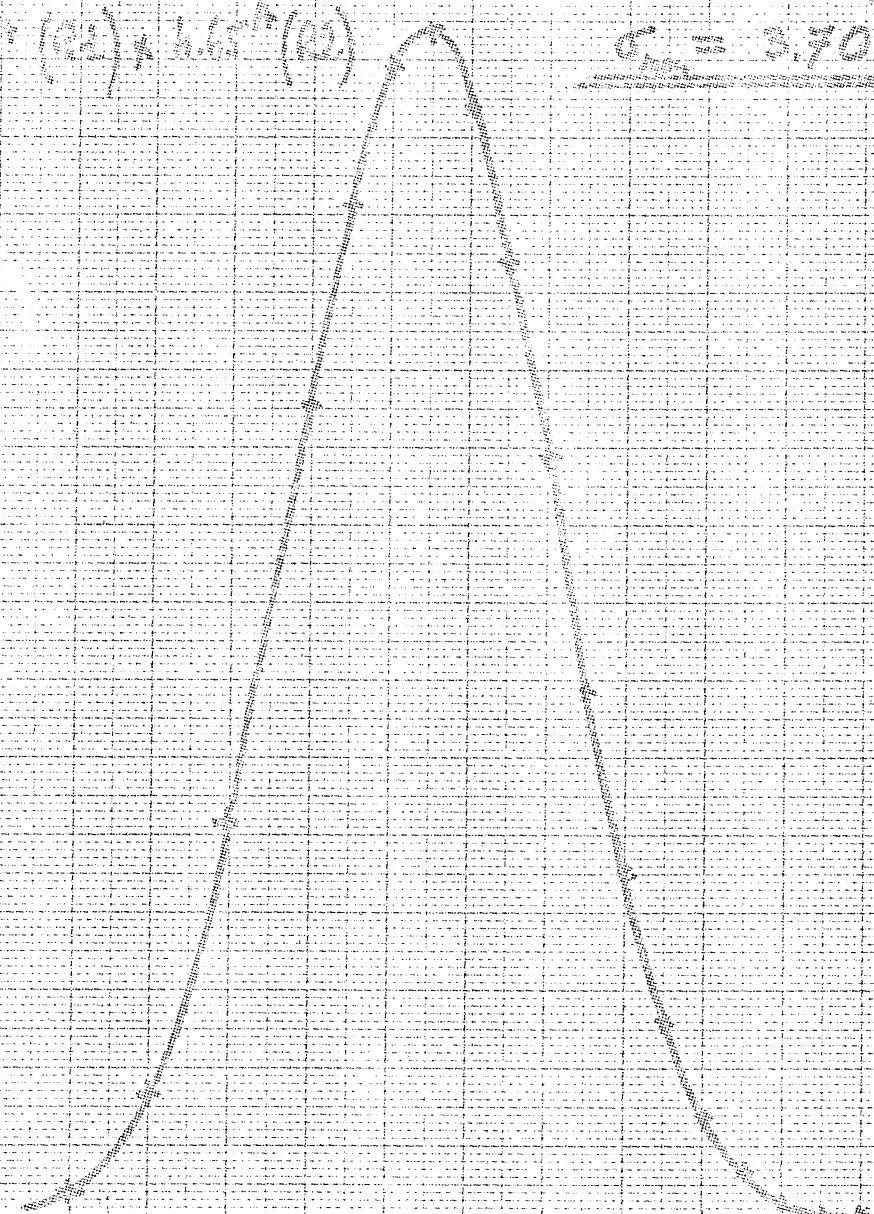
Handwritten calculations and values on the right side of the graph:
 $Area = 7.772 \text{ Count} \cdot \text{mm}$
 $L \cdot A = 2.05 \text{ mm}$
 $L = 1.04 \mu\text{m}^2/\text{sec}^2$
 $C_m = 3.70 \text{ nb}$

Handwritten label $1.00 \cdot 10^{-4} \text{ (sec)} \cdot 1.00 \cdot 10^{-4} \text{ (sec)}$ above the peak of the curve.

Y-axis labels: 1.0, 0.5, 1.0, 1.5, 2.0, 2.5, 3.0, 3.5, 4.0

X-axis labels: 0, 1, 2, 3, Diphot count (unc)

Handwritten text at the bottom of the page: "1.00 / sec" and "1.00 / sec".



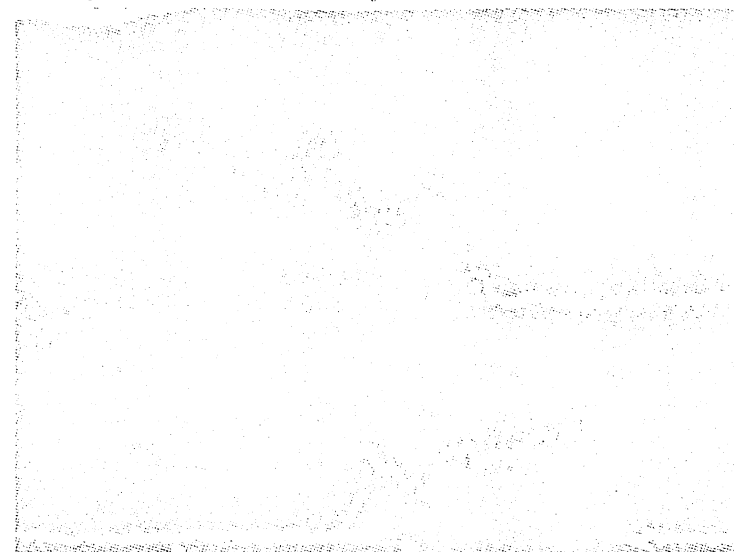
Longitudinal view $T_{p1} = 2.18''$ $T_{p2} = 1.14''$

0.75 0.85
↓ / 100, 100

0.75 0.85
↓

Longitudinal view $T_{p1} = 1.16''$ $T_{p2} = 1.21''$

0.75 0.85
↓ / 100, 100



Material by weight to volume %

Transverse vertical view

Ring 2 - $T_{p1} = 1.64''$

Material by weight to volume %

Transverse horizontal view

Ring 2 - $T_{p1} = 1.64''$



Transverse vertical view Material

Ring 2 - $T_{p1} = 12.216''$

0.75
↓

Transverse horizontal view Material

Ring 2 - $T_{p1} = 12.216''$